Starlight beneath the waves : in search of TeV photon emission from Gamma-Ray Bursts with the ANTARES Neutrino Telescope

Laksmana-Astraatmadja, T.

Part I

Theory

2 *The creation and propagation of TeV photons*

The high-energy component of the Band function hints at the nonthermal nature of the very high energy γ-ray emission. It has been shown that the extension of the spectrum towards the GeV regime has been established in some GRBs (e.g. Hurley et al. 1994; Abdo et al. 2009), while there are evidences that GRBs also emit TeV γ-rays (e.g. Atkins et al. 2000b; Poirier et al. 2003).

On the theoretical side, the emission of very high energy γ-rays are expected within the standard fireball shock scenario. The emission could occur from the leptonic component of the fireball through the electron inverse Compton mechanism as well as from the hadronic component through proton synchrotron, π^+ synchrotron emission and π^0 decay.

This Chapter will elaborate on the various mechanisms within the fireball shock scenario that could give emission of TeV γ-rays (Section 2.1) and the calculations employed to describe the spectrum of a GRB with its physical parameters such as its luminosity and its distance (Section 2.2). The annihilation of TeV γ-rays by ambient infrared photons will also be discussed, along with some discussions on how the optical depth is calculated and how this can affect our observations (Section 2.3).

2.1 *VHE γ-ray productions and the photon spectrum of a GRB*

Within the fireball of a GRB, the emission of VHE γ-rays could occur within external shocks as well as within internal shocks in the prompt phase. In the external shocks, the likely mechanism to emit VHE γ-rays is through electron Inverse Compton (IC) mechanism (Zhang & Mészáros, 2001) as well as through proton synchrotron emission (Vietri, 1997). Synchrotron emission within internal shocks could also produce VHE γ-rays up to 30 GeV (Pe'er & Waxman, 2004). Emission of VHE γ-rays in the prompt phase via the Synchrotron Self-Compton (SSC) mechanism can also be expected (Wang, Dai & Lu, 2001a,b).

These are not an exhaustive list of mechanisms that can occur,

and not all of the processes may be operative at any one time. For example, if the GRB wind is strongly dominated by a Poynting flux, γ-rays are emitted due to dissipation of magnetic energy (Lyutikov & Blandford, 2003) and the internal shock components would be suppressed or absent (Zhang & Mészáros, 2004).

Before we move on to the descriptions of some of these mechanisms, let us first define the following three reference frames and their notation:

1. The comoving frame or the wind rest frame is the frame of the outflowing ejecta expanding with bulk Lorentz factor Γ with respect to the observer and the central engine. Quantities measured in this frame are denoted with primes.

2. The source rest frame is the frame of the GRB central engine which is located at redshift z from the observer frame.

3. The observer frame is the reference frame of the observer on Earth, which is related to the source rest frame by the redshift correction factor $(1+z)$.

2.1.1 Synchrotron emission

IT IS NATURAL to think that the nonthermal emission of GRBs is caused by synchrotron emission, i.e. radiation from relativistic electrons gyrating in magnetic fields, if we consider the fireball scenario. In calculating the photon energy spectrum due to synchrotron radiation, we can first assume that the energy of the electrons are distributed according to a broken power-law function (Sari & Esin, 2001; Gupta & Zhang, 2007):

$$\frac{dN_e}{d\epsilon'_e} \propto \begin{cases} \epsilon'^{-p}_e, & \epsilon'_{e,\min} \leq \epsilon'_e \leq \epsilon'_{e,c}, \\ \epsilon'^{-(p+1)}_e, & \epsilon'_{e,c} < \epsilon'_e, \end{cases} \tag{2.1}$$

in the case of slow cooling, where p is the spectral index of the distribution function and $\epsilon'_{e,\min} = \gamma'_{e,\min} m_e c^2$ is the minimum injection energy of the electrons and $\gamma'_{e,\min}$ is the minimum Lorentz factor of the electron. Energies in the source rest frame and the comoving frame are related as $\epsilon = \Gamma\epsilon'$. To keep the energy of the electrons finite, the spectral index must obey $p > 2$. $\epsilon'_{e,c}$ is the

energy of an electron that loses its energy significantly during the dynamic timescale, defined as the cooling energy of the electrons.

If the electrons are cooling fast so that even the electrons with the minimum injection energy have cooled during the dynamical timescale, the electron distribution function is

$$\frac{dN_e}{d\epsilon'_e} \propto \begin{cases} \epsilon'^{-2}_e, & \epsilon'_{e,c} \leq \epsilon'_e \leq \epsilon'_{e,\min}, \\ \epsilon'^{-(p+1)}_e, & \epsilon'_{e,\min} < \epsilon'_e. \end{cases} \tag{2.2}$$

If the electrons are accelerated behind a relativistic shock propagating through a uniform cold medium with particle density n, the energy density U behind the shock is $U = 4\Gamma^2 n m_p c^2$, where Γ is the Lorentz factor of the shocked fluid (Sari, Piran & Narayan, 1998). The energy density is related to the GRB isotropic luminosity $L_{\rm iso}$ in the source frame by

$$U = \frac{L_{\rm iso}}{4\pi r_d^2 \Gamma^2 c}, \tag{2.3}$$

where $r_d = \delta t \Gamma^2 c$ is the radius of the γ-ray emitting region in the source frame and δt is the time variability of the GRB in the source frame.

If we further assume that a constant fraction ε_e and ε_p of the shock energy goes to the electrons and to the protons respectively, we would then obtain the minimum injection energy of the electrons in the comoving frame to be

$$\epsilon'_{e,\min} = \gamma'_{e,\min} m_e c^2 = \frac{\varepsilon_e}{\varepsilon_p} \left(\frac{p-2}{p-1} \right) m_p c^2 \Gamma. \tag{2.4}$$

We could also assume that the magnetic energy density behind the shock is a constant fraction ε_B of the shock energy, which would give us a magnetic field strength in the comoving frame (Sari, Piran & Narayan, 1998; Gupta & Zhang, 2007)

$$\begin{aligned} B' &= (32\pi m_p \xi \varepsilon_B n)^{1/2} \Gamma c \\ &\simeq 1.5 \times 10^7 \text{ G } \xi^{1/2} \varepsilon_B^{1/2} L_{\rm iso,51}^{1/2} \Gamma_{100}^{-3} \left(\frac{\delta t}{1 \text{ ms}} \right)^{-1}, \end{aligned} \tag{2.5}$$

where ξ is the compression ratio which is $\xi \sim 7$ for strong shocks (Gupta & Zhang, 2007), $L_{\rm iso,51} = L_{\rm iso}/(10^{51} \text{ erg s}^{-1})$, and $\Gamma_{100} = 10^{-2}\Gamma$.

Within the internal shocks, the total internal energy is distributed among electrons, protons, and the internal magnetic fields, and the relation $\varepsilon_e + \varepsilon_p + \varepsilon_B = 1$ is maintained.

The electrons will lose their energy through synchrotron radiation as well as inverse-Compton scattering (Panaitescu & Meszaros 1998, see also Subsection 2.1.2). The cooling energy $\epsilon'_{e,c}$ that breaks the electron energy spectrum can be calculated by first calculating the cooling time $t'_{\rm cool}$, which is a convolution of the cooling timescales for the synchrotron radiation t'_S and for the inverse-Compton (IC) scattering t'_{IC}:

$$\frac{1}{t'_{\rm cool}} = \frac{1}{t'_S} + \frac{1}{t'_{IC}}. \tag{2.6}$$

If U_e and U_B are the energy densities of electrons and magnetic fields respectively, the energy density of the synchrotron radiation is (Sari & Esin, 2001)

$$U_{e,\rm syn} = \frac{\eta_e U_e}{1+Y_e} = \frac{\eta_e \varepsilon_e U}{1+Y_e}, \tag{2.7}$$

here η_e is the radiation efficiency of the electron where $\eta_e = (\epsilon'_{e,c}/\epsilon'_{e,\rm min})^{2-p}$ for slow cooling and $\eta_e = 1$ for fast cooling, and

$$Y_e = \frac{L_{e,IC}}{L_{e,S}} = \frac{U_{e,\rm syn}}{U_B} = \frac{-1+\sqrt{1+4\eta_e\varepsilon_e/\varepsilon_B}}{2} \tag{2.8}$$

is the relative importance between the IC and synchrotron components. Here $L_{e,IC}$ and $L_{e,S}$ are the luminosities of the radiations emitted from inverse Compton radiation and synchrotron emission, respectively. The inverse of the cooling time of the electrons is then the ratio between the power and the electron energy (Gupta & Zhang, 2007)

$$\frac{1}{t'_{\rm cool}} = \frac{4}{3}\sigma_T \gamma'_{e,c} c \frac{(U_B + U_{e,\rm syn})}{m_e c^2} = \frac{4}{3}\sigma_T \gamma'_{e,c} \frac{c\varepsilon_B U}{m_e c^2}(1+Y_e), \tag{2.9}$$

where $\sigma_T = 6.625 \times 10^{-25}$ cm^{-2} is the Thomson cross section. If the ratio between the cooling timescale $t'_{\rm cool}$ and the dynamical timescale $t'_{\rm dyn} \simeq \Gamma\delta t$ is denoted as $f_c = t'_{\rm dyn}/t'_{\rm cool}$, the electron

cooling energy is then (Gupta & Zhang, 2007)

$$\begin{aligned}\epsilon'_{e,c} &= \gamma'_{e,c} m_e c^2 = m_e c^2 \frac{3 m_e c^2 f_c}{4\Gamma \delta t \sigma_T c U \varepsilon_B (1+Y_e)} \\ &= 5.3 \text{ keV} \left(\frac{\delta t}{1 \text{ ms}}\right) \left(\frac{f_c}{100}\right) \Gamma_{100}^5 L_{\text{iso},51}^{-1} \varepsilon_B^{-1} (1+Y_e)^{-1}.\end{aligned} \tag{2.10}$$

The cooling energy $\epsilon'_{e,c}$ and the minimum injection energy $\epsilon'_{e,\min}$ of the electrons define two break energies in the photon spectrum due to synchrotron spectrum. The cooling break energy in the photon spectrum is (Gupta & Zhang, 2007)

$$\begin{aligned}\epsilon_{\gamma,c,S} &= \Gamma \frac{3h}{4\pi} \left(\frac{\epsilon'_{e,c}}{m_e c^2}\right)^2 \frac{eB'c}{m_e c^2} \\ &\simeq 2.8 \text{ meV} \left(\frac{\delta t}{1 \text{ ms}}\right)^{1/2} \left(\frac{f_c}{100}\right)^2 \xi^{1/2} L_{\text{iso},51}^{-3/2} \varepsilon_B^{-3/2} \Gamma_{100}^8 (1+Y_e)^{-2}.\end{aligned} \tag{2.11}$$

We can see that $\epsilon_{\gamma,c,S}$ is very sensitive mainly to Γ, allowing it to become very large at the slightest increase of the bulk Lorentz factor.

The break energy in the photon spectrum due to the minimum electron injection energy is then

$$\begin{aligned}\epsilon_{\gamma,\min,S} &= \Gamma \frac{3h}{4\pi} \left(\frac{\epsilon'_{e,\min}}{m_e c^2}\right)^2 \frac{eB'c}{m_e c^2} \\ &\simeq 85 \text{ MeV} \left(\frac{\varepsilon_e}{\varepsilon_p}\right)^2 \left(\frac{\delta t}{1 \text{ ms}}\right)^{-1} (\xi \varepsilon_B L_{\text{iso},51})^{1/2} \Gamma_{100}^{-1}.\end{aligned} \tag{2.12}$$

Synchrotron radiation is also accompanied by absorption, in which radiated photons interact with a charge in magnetic fields and are absorbed, transferring its energy to the charge. This is called synchrotron self-absorption (Rybicki & Lightman, 1979). The synchrotron self-absorption (SSA) energy ϵ_{SSA} within internal shocks will constitute the minimum cutoff in the photon energy spectrum, and can be expressed as (Gupta & Zhang, 2007)

$$\epsilon_{\text{SSA}} \simeq 3.57 \text{ keV} \left(\frac{\delta t}{1 \text{ ms}}\right)^{-5/7} L_{\text{iso},51}^{5/14} \Gamma_{100}^{-8/7} (\xi \varepsilon_B)^{1/14} \left(\frac{\varepsilon_e \eta_e}{1+Y_e}\right)^{2/7}. \tag{2.13}$$

The photon energy spectrum due to synchrotron radiation for the case of slow-cooling relativistic electrons is then (Sari, Piran & Narayan, 1998; Gupta & Zhang, 2007)

$$\left.\frac{dN_\gamma}{d\epsilon_\gamma}\right|_S \propto \begin{cases} \epsilon_\gamma^{-2/3}, & \epsilon_{\rm SSA} < \epsilon_\gamma \leq \epsilon_{\gamma,{\rm min},S}, \\ \epsilon_{\gamma,{\rm min},S}^{-2/3+(p+1)/2}\epsilon_\gamma^{-(p+1)/2}, & \epsilon_{\gamma,{\rm min},S} < \epsilon_\gamma \leq \epsilon_{\gamma,c,S}, \\ \epsilon_{\gamma,{\rm min},S}^{-2/3+(p+1)/2}\epsilon_{\gamma,c,S}^{1/2}\epsilon_\gamma^{-(p+2)/2}, & \epsilon_{\gamma,c,S} < \epsilon_\gamma. \end{cases} \tag{2.14}$$

The slow-cooling case happens when $\epsilon_{e,c,S} > \epsilon_{e,{\rm min},S}$. For the case of fast-cooling electrons, i.e. $\epsilon_{e,c,S} < \epsilon_{e,{\rm min},S}$, the spectrum will be

$$\left.\frac{dN_\gamma}{d\epsilon_\gamma}\right|_S \propto \begin{cases} \epsilon_\gamma^{-2/3}, & \epsilon_{\rm SSA} < \epsilon_\gamma \leq \epsilon_{\gamma,c,S}, \\ \epsilon_{\gamma,c,S}^{5/6}\epsilon_\gamma^{-3/2}, & \epsilon_{\gamma,c,S} < \epsilon_\gamma \leq \epsilon_{\gamma,{\rm min},S}, \\ \epsilon_{\gamma,c,S}^{5/6}\epsilon_{\gamma,{\rm min},S}^{-3/2+(p+2)/2}\epsilon_\gamma^{-(p+2)/2}, & \epsilon_{\gamma,{\rm min},S} < \epsilon_\gamma. \end{cases} \tag{2.15}$$

As we can see, the photon energy spectrum consists of three segments. The low-energy part of the spectrum will always be the sum of the contribution of the tails of the emission of all electrons and thus is independent of the exact shape of the electron distribution. On the other hand, at the highest energy the most energetic electrons cool rapidly and practically transfer all their energy to the photons. Thus the high-energy part of the spectrum will have a power-law function that depends on the energy spectrum of the electrons.

Within the internal shock scenario, the total energy emitted in synchrotron radiation is $E_{\rm iso}\eta_e\varepsilon_e(1+Y_e)$. Here $E_{\rm iso}$ is the total energy emitted by the GRB which is related to the luminosity $L_{\rm iso}$ by $E_{\rm iso} = L_{\rm iso}T_{90}/(1+z)$, where T_{90} is the duration of the burst in the observer frame. The normalisation constant $f_{\gamma,S}$ for the synchrotron photon energy spectrum can then be calculated:

$$f_{\gamma,S}\int_{\epsilon_{\rm SSA}}^{\epsilon_{\gamma,{\rm max},S}} d\epsilon_\gamma\epsilon_\gamma \left.\frac{dN_\gamma}{d\epsilon_\gamma}\right|_S = E_{\rm iso}\frac{\eta_e\varepsilon_e}{(1+Y_e)}, \tag{2.16}$$

where the maximum photon energy that can be radiated is (Gupta & Zhang, 2007)

$$\epsilon_{\gamma,{\rm max},S} = 102\ {\rm GeV}\ \left(\frac{\Gamma_{100}}{1+Y_e}\right). \tag{2.17}$$

2.1.2 *Electron inverse-Compton scattering*

In inverse Compton (IC) scattering, ultrarelativistic electrons scatter low-energy ambient photons so that the photons gain energy at the expense of the electrons which subsequently lose their energy.

Assuming a spatially isotropic and homogeneous distribution of electrons and photons, the spectrum of accelerated photons per unit time per unit energy is (Blumenthal & Gould, 1970; Gupta & Zhang, 2007)

$$\left.\frac{dN}{d\epsilon_\gamma}\right|_{IC} = \int\int d\epsilon_e d\varepsilon_\gamma W(\epsilon_e, \varepsilon_\gamma, \epsilon_\gamma) \frac{dN_e}{d\epsilon_e} \left.\frac{dN_\gamma}{d\varepsilon_\gamma}\right|_S, \tag{2.18}$$

where

$$W(\epsilon_e, \varepsilon_\gamma, \epsilon_\gamma) = \frac{8\pi r_e^2 c}{\epsilon_e \eta} \left[2q \ln q + (1-q)\left(1 + 2q + \frac{\eta^2 q^2}{2(1+\eta q)}\right)\right], \tag{2.19}$$

and

$$\eta = \frac{4\varepsilon_\gamma \epsilon_e}{(m_e c^2)^2}, \quad q = \frac{\epsilon_\gamma}{\eta(\epsilon_e - \epsilon_\gamma)}. \tag{2.20}$$

Here $W(\epsilon_e, \varepsilon_\gamma, \epsilon_\gamma)$ defined in Equation 2.19 is the scattering probability which already take into account the Klein-Nishina effect. The parameter η in Equation 2.20 defines the domain of the scattering: For $\eta \ll 1$ the photons take only a small fraction of the electron energy and thus scatterings occur in the Thomson regime, while for $\eta \gg 1$ the photons take almost all the energy of the electrons in one scattering, which is called the Klein-Nishina regime.

Solving the integrals in Equation 2.18, the photon energy spectrum due to inverse-Compton scattering for slow-cooling of electrons is (Gupta & Zhang, 2007)

$$\left.\frac{dN_\gamma}{d\epsilon_\gamma}\right|_{IC} \propto \begin{cases} \epsilon_\gamma^{-2/3}, & \epsilon_{\mathrm{SSA},IC} < \epsilon_\gamma \le \epsilon_{\gamma,\mathrm{min},IC}, \\ \epsilon_{\gamma,\mathrm{min},IC}^{-2/3+(p+1)/2} \epsilon_\gamma^{-(p+1)/2}, & \epsilon_{\gamma,\mathrm{min},IC} < \epsilon_\gamma \le \epsilon_{\gamma,c,IC}, \\ \epsilon_{\gamma,\mathrm{min},IC}^{-2/3+(p+1)/2} \epsilon_{\gamma,c,IC}^{1/2} \epsilon_\gamma^{-(p+2)/2}, & \epsilon_{\gamma,c,IC} < \epsilon_\gamma \le \epsilon_{\gamma,K}, \\ \epsilon_{\gamma,\mathrm{min},IC}^{-2/3+(p+1)/2} \epsilon_{\gamma,c,IC}^{1/2} \epsilon_{\gamma,K}^{(p-2)/2} \epsilon_\gamma^{-p}, & \epsilon_{\gamma,K} < \epsilon_\gamma \end{cases} \tag{2.21}$$

Here the break energies for the IC emission are related to the break energies for the synchrotron emission by the electron Lorentz factor $\gamma'_{e,\min}$ and $\gamma'_{e,c}$: $\epsilon_{\mathrm{SSA},IC} = \gamma'^2_{e,\min}\epsilon_{\mathrm{SSA}}$, $\epsilon_{\gamma,\min,IC} = \gamma'^2_{e,\min}\epsilon_{\gamma,\min}$, and $\epsilon_{\gamma,c,IC} = \gamma'^2_{e,c}\epsilon_{\gamma,c}$. In the case of fast cooling, where $\epsilon_{\gamma,\min,IC} > \epsilon_{\gamma,c,IC}$, the IC photon spectrum becomes

$$\left.\frac{dN_\gamma}{d\epsilon_\gamma}\right|_{IC} \propto \begin{cases} \epsilon_\gamma^{-2/3}, & \epsilon_{\mathrm{SSA},IC} < \epsilon_\gamma \leq \epsilon_{\gamma,c,IC}, \\ \epsilon_{\gamma,c,IC}^{5/6}\epsilon_\gamma^{-3/2}, & \epsilon_{\gamma,c,IC} < \epsilon_\gamma \leq \epsilon_{\gamma,\min,IC}, \\ \epsilon_{\gamma,c,IC}^{5/6}\epsilon_{\gamma,\min,IC}^{(p-1)/2}\epsilon_\gamma^{-(p+2)/2}, & \epsilon_{\gamma,\min,IC} < \epsilon_\gamma \leq \epsilon_{\gamma,K}, \\ \epsilon_{\gamma,c,IC}^{5/6}\epsilon_{\gamma,\min,IC}^{(p-1)/2}\epsilon_{\gamma,K}^{(p-2)/2}\epsilon_\gamma^{-p}, & \epsilon_{\gamma,K} < \epsilon_\gamma. \end{cases} \tag{2.22}$$

Contrary to Equation 2.21, in Equation 2.22 the relation between the break IC energies with the break synchrotron energies are $\epsilon_{\mathrm{SSA},IC} = \gamma'^2_{e,c}\epsilon_{\mathrm{SSA}}$, $\epsilon_{\gamma,c,IC} = \gamma'^2_{e,c}\epsilon_{\gamma,c}$, and $\epsilon_{\gamma,\min,IC} = \gamma'^2_{e,\min}\epsilon_{\gamma,\min}$.

In both Equations, $\epsilon_{\gamma,K}$ is the energy at which IC scattering enters the Klein-Nishina (KN) regime and the KN effect becomes important (Fragile et al., 2004):

$$\epsilon_{\gamma,K} = 2.5\ \mathrm{GeV}\ \left(\frac{\epsilon_{\gamma,\mathrm{pk}}}{1\ \mathrm{MeV}}\right)^{-1} \Gamma_{100}^2, \tag{2.23}$$

here $\epsilon_{\gamma,\mathrm{pk}} = \max\left[\epsilon_{\gamma,c,S}, \epsilon_{\gamma,\min,S}\right]$ is the energy at which the synchtroton spectrum peaks.

As the electrons scatter the ambient photons, they will lose their energy and cool down to a level in which they could no longer scatter photons. The timescale of the cooling is (Fragile et al., 2004)

$$t'_{IC} = 1.1 \times 10^{-5}\ \mathrm{s}\ \left(\frac{\delta t}{1\ \mathrm{ms}}\right)^2 \Gamma_{100}^6 \left(\gamma'_e L_{\mathrm{iso},51}\right)^{-1}. \tag{2.24}$$

The cooling of the electrons would naturally impose a cutoff in the resulting IC γ-ray spectrum at maximum photon energy (Fragile et al., 2004)

$$\epsilon_{\gamma,\max,IC} = 852\left(\frac{\delta t}{1\ \mathrm{ms}}\right)^{1/2} \frac{\Gamma_{100}^{5/2}}{\varepsilon_B^{1/4} L_{\mathrm{iso},51}^{1/4}}\ \mathrm{GeV}. \tag{2.25}$$

Knowing the maximum energy of the photons emitted by IC scattering, the IC photon spectrum can then be normalized by (Gupta

& Zhang, 2007)

$$f_{\gamma,IC}\int_{\epsilon_{\mathrm{SSA},IC}}^{\epsilon_{\gamma,\mathrm{max},IC}} d\epsilon_\gamma \epsilon_\gamma \left.\frac{dN_\gamma}{d\epsilon_\gamma}\right|_{IC} = E_{\mathrm{iso}}\frac{\eta_e \varepsilon_e Y_e}{(1+Y_e)}. \tag{2.26}$$

The most likely origin for an extendend high-energy afterglow component in GeV energies is from the electron IC scattering in the external shock (Zhang & Mészáros, 2001). In general, the detectability of the IC component is favoured by a high-density external medium, and it is possible that the late GeV emission occured in GRB 940217 (Hurley et al., 1994) was caused by the IC component.

2.1.3 *Proton synchrotron emission*

There are two ways in which relativistic protons lose their energy. The first is by synchrotron emission and the second is—as mentioned in Chapter 1—by interacting with low-energy photons in the ambient medium to produce Delta resonances. The Delta resonances will subsequently decay into photopions (π^0, π^+). The probabilities of π^0 and π^+ production are $1/3$ and $2/3$, respectively. π^0s primarily decay into γ-rays, i.e. $\pi^0 \rightarrow \gamma\gamma$, while π^+s decay into neutrinos (Equations 1.2–1.3). VHE γ-rays production from photopions will be discussed later-on in the next subsection, however since photopion productions affect proton synchrotron emission, some of the properties related to photopion production will also be discussed here.

The emission of VHE γ-rays from proton synchtroton was originally proposed by Vietri (1997). Vietri argued that cosmic rays of energies $\sim 10^{20}$ eV could be produced from external shocks, and these protons could emit VHE γ-rays through synchrotron emission as they cross the acceleration region.

To calculate the photon energy spectrum due to proton synchrotron, let us first assume—analogous to electron synchtroton emission—that the energy of the protons is distributed in a power-law function:

$$\frac{dN_p}{d\epsilon'_p} \propto \begin{cases} \epsilon_e'^{-p}, & \epsilon'_{p,\mathrm{min}} \leq \epsilon'_p \leq \epsilon'_{p,c}, \\ \epsilon_e'^{-(p+1)}, & \epsilon'_{p,c} < \epsilon'_p, \end{cases} \tag{2.27}$$

here $\epsilon_{p,\min} = \gamma'_{p,\min} m_p c^2 (p-2)/(p-1)$ is the minimum injection energy of the protons and $\epsilon'_{p,c}$ is the break energy in the spectrum due to proton cooling. In this calculation only the slow-cooling scenario is considered since protons are poor emitters of photons.

The break energy of the proton spectrum can be calculated by comparing the comoving dynamical timescale $t'_{\rm dyn}$ with the cooling timescale $t'_{\rm cool}$ of the protons. The inverse of the cooling timescale $t'_{\rm cool}$ is equal to

$$\frac{1}{t'_{\rm cool}} = \frac{1}{t'_{\rm S}} + \frac{1}{t'_{\pi}}, \tag{2.28}$$

where t'_{π} is the photopion cooling timescale which is equal to $1/t'_{\pi} \sim f_{\pi}/t'_{\rm dyn}$. Here f_{π} is the fraction of the proton energy that goes into pion production in $p\gamma$ interactions. The cooling time due to photopion productions has been calculated by Waxman & Bahcall (1997) for the calculation of neutrino energy spectrum:

$$\begin{aligned} \frac{1}{t'_{\pi}} &\equiv -\frac{1}{\epsilon_p}\frac{d\epsilon_p}{dt} \\ &= \frac{c}{2\gamma'^2_p}\int_{\epsilon_0}^{\infty} d\epsilon \sigma_{\pi}(\epsilon)\xi(\epsilon)\epsilon \int_{\epsilon/2\gamma'_p}^{\infty} \frac{d\epsilon_\gamma}{\epsilon_\gamma^2}\frac{dN_\gamma}{d\epsilon_\gamma}, \end{aligned} \tag{2.29}$$

where $\gamma'_p = \epsilon_p/m_p c^2$, $\sigma_{\pi}(\epsilon)$ is the cross section for pion production for a photon with energy ϵ in the proton rest frame, $\xi(\epsilon)$ is the average fraction of energy lost to the pion, and $\epsilon_0 = 0.15$ GeV is the threshold energy. The second integral is over the low-energy spectrum where $dN_\gamma/d\epsilon_\gamma$ is the photon spectrum of the GRB in the frame of the protons. The solution to this integral is (Waxman & Bahcall, 1997)

$$\frac{1}{t'_{\pi}} \simeq \frac{U_\gamma}{2\epsilon_{\gamma b}} c\sigma_{p\gamma}\xi_{\rm peak}\frac{\Delta\epsilon}{\epsilon_{\rm peak}}\min(1, 2\gamma'_p\epsilon_{\gamma b}/\epsilon_{\rm peak}), \tag{2.30}$$

where $\sigma_{p\gamma} \simeq 5 \times 10^{-28}$ cm^{-2} is the peak value of the $p\gamma$ interaction cross section at the Delta resonance and $\xi_{\rm peak} \simeq 0.2$ is the value of σ and ξ at $\epsilon = \epsilon_{\rm peak} \sim 0.3$ GeV and $\Delta\epsilon \simeq 0.2$ GeV is the width of the peak.

Using the relation between photon luminosity and the photon energy density shown in Equation 2.3, the fraction of energy lost

by protons to pions can be calculated:

$$f_\pi(\epsilon_p) \simeq \frac{\Gamma \delta t}{t'_\pi} = f_0 \begin{cases} \frac{\epsilon_p}{\epsilon_{pb}}, & \epsilon_p \leq \epsilon_{pb}, \\ 1, & \epsilon_p > \epsilon_{pb}, \end{cases} \tag{2.31}$$

where

$$f_0 = 16.2 \frac{L_{\rm iso,51}}{\Gamma_{100}^4} \left(\frac{\epsilon_{\gamma b}}{1\ {\rm MeV}}\right)^{-1} \left(\frac{\delta t}{1\ {\rm ms}}\right)^{-1}. \tag{2.32}$$

Here $\epsilon_{\gamma b}$ is the break energy of the Band spectrum. In this formula the spectral indices of the Band function is assumed to be $(\alpha, \beta) = (1, 2)$. A more general formula can be found in Gupta & Zhang (2007). The proton break energy in Equation 2.31 is

$$\epsilon_{pb} = 3 \times 10^3\ \Gamma_{100}^2 \left(\frac{\epsilon_{\gamma b}}{1\ {\rm MeV}}\right)^{-1}\ {\rm TeV}. \tag{2.33}$$

The break energy $\epsilon'_{p,c}$ in the proton spectrum due to proton cooling can be calculated by similar mean as in the previous section for the case of electrons:

$$\epsilon'_{p,c} = 6.25 \times 10^4\ {\rm TeV}\ \left(\frac{f_c}{100}\right) \left(\frac{\delta t}{1\ {\rm ms}}\right) \left(\frac{\Gamma_{100}^6}{\varepsilon_B \Gamma_{100} + 1.51}\right) L_{\rm iso,51}^{-1}. \tag{2.34}$$

The photon energy spectrum from proton synchrotron is then (Gupta & Zhang, 2007)

$$\left.\frac{dN_\gamma}{d\epsilon_\gamma}\right|_{PS} \propto \begin{cases} \epsilon_\gamma^{-(p+1)/2}, & \epsilon_{\gamma,{\rm min},PS} < \epsilon_\gamma \leq \epsilon_{\gamma,c,PS}, \\ \epsilon_\gamma^{3/2} \epsilon_\gamma^{-(p+2)/2}, & \epsilon_{\gamma,c,PS} < \epsilon_\gamma, \end{cases} \tag{2.35}$$

here the minimum photon energy from proton synchrotron emission is related to the minimum photon energy from electron synchtroton by (Zhang & Mészáros, 2001)

$$\epsilon_{\gamma,{\rm min},PS} = \epsilon_{\gamma,{\rm min},S} \left(\frac{\epsilon'_{p,{\rm min}}}{\epsilon'_{e,{\rm min}}}\right)^2 \left(\frac{m_e}{m_p}\right)^3. \tag{2.36}$$

The cooling break energy $\epsilon_{\gamma,c,PS}$ in the photon spectrum is the characteristic photon energy for proton of energy $\epsilon'_{p,c}$. It can be expressed as (Fragile et al., 2004)

$$\epsilon_{\gamma,c,PS} = 0.32\ {\rm eV}\ \left(\frac{\delta t}{1\ {\rm ms}}\right) \Gamma_{100}^8 (\varepsilon_B L_{\rm iso,51})^{-3/2}. \tag{2.37}$$

To normalize the photon spectrum, the contribution of proton synchrotron relative to $p\gamma$ interactions must be calculated. Similar to the calculation of Y_e, we can define (Gupta & Zhang, 2007)

$$Y_p = \frac{L_{p,p\gamma}}{L_{p,PS}} = \frac{\sigma_{p\gamma}}{\sigma_{p,T}} \frac{U_{e,S}}{U_B} = \frac{\sigma_{p\gamma}}{\sigma_{p,T}} Y_e, \tag{2.38}$$

where $L_{p,p\gamma}$ and $L_{p,PS}$ are the luminosities emitted in $p\gamma$ and proton synchrotron respectively and $\sigma_{p,T} = (m_e/m_p)^2 \sigma_{e,T}$ is the Thomson cross section for protons. Since $\sigma_{p\gamma}$ is much larger than $\sigma_{p,T}$, most of the proton energy will go to the $p\gamma$ interaction rather than to the proton synchrotron emission. The normalisation of the proton synchrotron photon spectrum is then

$$f_{\gamma,PS} \int_{\epsilon_{\gamma,\min,PS}}^{\epsilon_{\gamma,\max,PS}} d\epsilon_\gamma \epsilon_\gamma \left. \frac{dN_\gamma}{d\epsilon_\gamma} \right|_{PS} = E_{\rm iso} \frac{\eta_p \varepsilon_p}{(1+Y_p)}, \tag{2.39}$$

where $\eta_p = (\epsilon'_{p,c}/\epsilon'_{p,\min})^{2-\alpha}$. Proton acceleration is also limited by synchrotron cooling which limits the maximum proton energy that can be achieved by proton acceleration (Totani, 1998a):

$$\epsilon_{p,\max,PS} = 4.26 \times 10^{17} \text{ eV} \left(\frac{\delta t}{1 \text{ ms}} \right)^{1/2} (\varepsilon_B L_{\rm iso,51})^{-1/4} \Gamma_{100}^{5/2}, \tag{2.40}$$

which again imposes a cutoff in the resulting photon spectrum:

$$\epsilon_{\gamma,\max,PS} \simeq 5\Gamma_{300} \text{ TeV}. \tag{2.41}$$

Within the external shock scenario, already early-on Gallant & Achterberg (1999) showed the difficulty of accelerating protons in a fireball expanding into the ambient interstellar medium. For ambient Fermi-accelerated particles with initialy isotropic momenta, they can gain a factor of $\sim\Gamma^2$ in energy in the first shock crossing cycle but only a factor of 2 in the subsequent shocks, because the particles do not have time to become isotropic before being overtaken by the shock. This is in contradiction with the assumption of Vietri (1997) that the energy of the accelerated particle is multiplied by a factor of Γ^2 after each shock crossing. Under the conditions imposed by Gallant & Achterberg (1999) the maximum energy attainable is well below 10^{20} eV. To solve this problem, Gallant & Achterberg (1999) suggested that the shock expands into an already-relativistic medium such as the pulsar wind bubble.

Pulsars emit relativistic winds which should contain ions. These relativistic ions conserve their post-shock energy throughout a relativistic plasma bubble formed from the shock of the pulsar wind against the ambient gas. The presence of a pulsar wind bubble surrounding the GRB progenitor is plausible in the neutron-star-binary merger scenario.

2.1.4 π^0 decay

FOR TYPICAL parameters of a GRB, a significant fraction of the energy of the protons accelerated to energies larger than the break energy, $\epsilon_{pb}^{\rm ob} \sim 10^4$ TeV, would be lost to pion production. π^0s typically carry $\xi_{\rm peak} \sim 20\%$ of the proton's energy and in the center of mass frame the γ-rays produced in the decay will equally share the available energy. The mean pion energy is then $\langle \epsilon_{\pi^0} \rangle \sim \xi_{\rm peak} \epsilon_p$, and as the energy of the neutral pions will be shared equally among the γ-rays, each γ-ray will then have an average energy $\langle \epsilon_\gamma \rangle \sim 0.5 \xi_{\rm peak} \epsilon_p$.

Assuming a photon with energy $2 m_e c^2 \sim 1$ MeV in the comoving frame, then in the source rest frame the energy of the photon is 400 MeV for $\Gamma = 400$. This photon could produce photopions by interacting with protons of minimum energy $\epsilon_p \sim 120$ TeV (Gupta & Zhang, 2007). The minimum energy of the photons produced from π^0 is then expected to be $\langle \epsilon_\gamma \rangle \sim 12$ TeV.

The γ-ray spectrum due to π^0 decay can be calculated, using the proton energy spectrum defined in Equation 2.27 and assuming the fraction $f_\pi/3$ of the protons' energy goes into π^0 (Fragile et al., 2004; Gupta & Zhang, 2007):

$$\left.\frac{dN_\gamma}{d\epsilon_\gamma}\right|_{\pi^0} \propto \frac{1}{3}\frac{f_\pi(\epsilon_\gamma)}{2} \begin{cases} \epsilon_\gamma^{2-p}, & \epsilon_\gamma \leq \epsilon_{\gamma,c,\pi^0}, \\ \epsilon_\gamma^{1-p}, & \epsilon_\gamma > \epsilon_{\gamma,c,\pi^0}, \end{cases} \tag{2.42}$$

where the break energy $\epsilon_{\gamma,c,\pi^0}$ in the γ-ray spectrum due to pion decay is $\epsilon_{\gamma,c,\pi^0} = 0.5 \xi_{\rm peak} \epsilon_{pb}$. The photon flux due to pion decay can then be normalized by

$$f_{\gamma,\pi^0} \int_{\epsilon_{\gamma,\min,\pi^0}}^{\epsilon_{\gamma,\max,\pi^0}} d\epsilon_\gamma \epsilon_\gamma \left.\frac{dN_\gamma}{d\epsilon_\gamma}\right|_{\pi^0} = \frac{1}{3} E_{\rm iso} \frac{\eta_p \varepsilon_p Y_p}{(1+Y_p)}, \tag{2.43}$$

where $\epsilon_{\gamma,\min,\pi^0} = 30\Gamma$ GeV and $\epsilon_{\gamma,\max,\pi^0} = 0.1 \epsilon_{p,\max,PS}$.

2.1.5 *Internal absorption of VHE γ-rays by low-energy photons*

In the internal shock, γ-rays produced from the mechanisms described in previous subsections will interact with low-energy photons through the $\gamma\gamma \to e^+e^-$ process, annihilating themselves and creating electron-positron pairs. A γ-ray with energy ϵ_γ can produce a pair of electron-positron if it impacts a photon with threshold energy

$$\epsilon_{\rm th} = \frac{2\epsilon_e^2}{\epsilon_\gamma(1-\mu_i)}, \tag{2.44}$$

where $\mu_i = \cos\theta_i$, and θ_i is the angle of impact between the two photons. For head-on collisions, the energy of the photons which will interact with passing γ-ray photons is then

$$\epsilon_{\rm th} = 0.261 \left(\frac{1\ {\rm TeV}}{\epsilon_\gamma}\right)\ {\rm eV}. \tag{2.45}$$

The cross section of the $\gamma\gamma$ pair-production for photons of energies (ϵ_1, ϵ_2) is (Breit & Wheeler, 1934; Gould & Schréder, 1967)

$$\begin{aligned}\sigma(\epsilon_1,\epsilon_2,\mu_i) = {} & \tfrac{3}{16}\sigma_T(1-\beta^2) \\ & \times \left[(3-\beta^4)\ln\left(\frac{1+\beta}{1-\beta}\right) + 2\beta(\beta^2-2)\right],\end{aligned} \tag{2.46}$$

in which σ_T is the Thomson cross section and β is the electron-positron velocity in the center-of-mass frame:

$$\beta = \sqrt{1 - \frac{2\epsilon_e^2}{\epsilon_1\epsilon_2(1-\mu_i)}}. \tag{2.47}$$

The mean free path $l_{\gamma\gamma}$ of a γ-ray with energy ϵ'_γ interacting with low-energy photon of energy ϵ'_L can then be calculated as (Gould & Schréder, 1967)

$$l^{-1}_{\gamma\gamma}(\epsilon'_\gamma) = \int_{-1}^{1} d\mu_i(1-\mu_i)\int_{\epsilon'_{\rm th}}^{\infty} d\epsilon'_L \frac{dN_\gamma}{d\epsilon'_L}\sigma_{\gamma\gamma}(\epsilon'_\gamma,\epsilon'_L,\mu_i). \tag{2.48}$$

The low-energy photon spectrum is already known and is observed by BATSE and *Swift* as the Band spectrum. Theoretically this corresponds to the electron synchrotron component (Gupta & Zhang, 2007), which is related to the luminosity by

$$\int_{\epsilon'_{\rm SSA}}^{\epsilon'_{\gamma,{\rm max,S}}} d\epsilon'_L\epsilon'_L\frac{dN_\gamma}{d\epsilon'_\gamma} = U_\gamma. \tag{2.49}$$

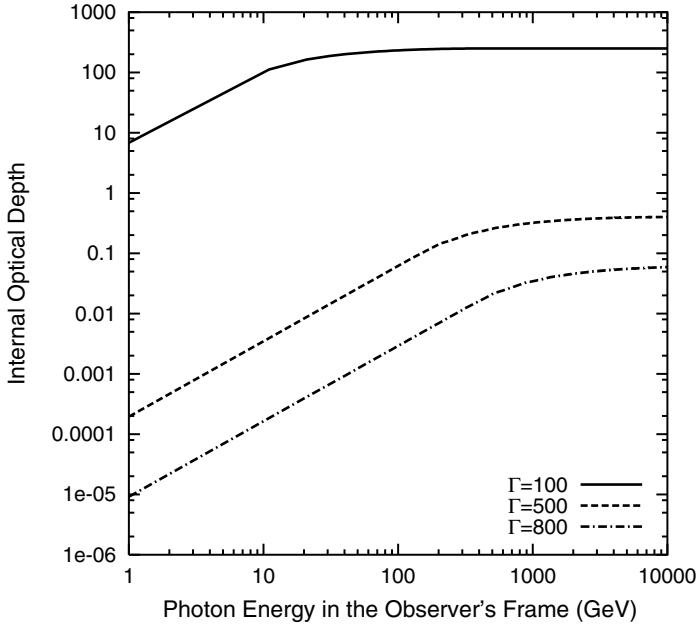

Figure 2.1: A plot of the internal optical depth $\tau_{\gamma\gamma,\mathrm{int}}$ as a function of energy in the observer frame, for different values of bulk Lorentz factor Γ, while all other values are kept the same. Here $L_{\mathrm{iso}} = 10^{51}$ erg s^{-1}, $(\alpha, \beta) = (1, 2.25)$, $\epsilon_{\gamma b} = 500$ keV, $\delta = 500$ ms, and $z = 0.1$. Figure reproduced from Bhattacharjee & Gupta (2003).

The integral in Equation 2.48 has been analytically solved by Baring & Harding (1997) and Bhattacharjee & Gupta (2003), and the internal optical depth is then

$$\tau_{\gamma\gamma,\mathrm{int}}(\epsilon'_\gamma) = \frac{r_d}{\Gamma} l^{-1}_{\gamma\gamma}(\epsilon'_\gamma). \tag{2.50}$$

An example of how $\tau_{\gamma\gamma,\mathrm{int}}$ varies with observed γ-ray energy and Lorentz factor Γ is shown in Figure 2.1. As we can see, there is a high dependence of $\tau_{\gamma\gamma,\mathrm{int}}$ on the Lorentz factor Γ, which in turn will determine how compact the fireball is. The compactness of the fireball can be defined as $l' = \Delta R n'_\gamma \sigma_T$, where $\Delta R = c t_{\mathrm{dyn}}$ is the comoving width and $n'_\gamma = \varepsilon_e L_{\mathrm{iso}} / (4\pi m_e c^3 \Gamma^2 r_d^2)$ is the comoving number density of photons of energy larger than the electron's rest mass, $\epsilon_\gamma \geq m_e c^2$ (Pe'er & Waxman, 2004). The compactness parameter is thus

$$l' = \frac{\varepsilon_e L_{\mathrm{iso}} \sigma_T}{16\pi m_e c^4 \Gamma^5 \Delta t} = 2500 \left(\frac{\delta t}{1\ \mathrm{ms}}\right)^{-1} L_{\mathrm{iso},51} \varepsilon_e \Gamma^{-5}_{100}. \tag{2.51}$$

A source with low Lorentz factor will then make the fireball very compact and increase the internal optical depth $\tau_{\gamma\gamma,\mathrm{int}}$. According

to Pe'er & Waxman (2004), who performed a fully numerical treatment to the calculation of GRB prompt emissions, a fireball with large compactness parameter (small Γ), $l' > 100$, should present a sharp cutoff in the photon spectra at $\epsilon_\gamma \sim 10$ MeV. A small-to-moderate compactness parameter (large Γ), $l' \lesssim 10$, would extend the spectra to $\epsilon_\gamma \sim 10$ GeV. For fireballs with moderate-to-large compactness parameters, we could then expect a rapid expansion of the fireball and the escape of TeV γ-rays from the fireball, which could be observed as the VHE component of the prompt emission.

THE ENERGIES carried by the electron-positron pairs could be converted and re-radiated again as photons through either the $e^+e^- \rightarrow \gamma\gamma$ process or through synchrotron emission. Calculations by Pe'er & Waxman (2004) and Gupta & Zhang (2007) shows that this feedback process does not contribute significantly to the resulting photon spectrum for fireballs with low compactness parameter. However, in fireballs with high compactness parameter, annihilations of electron-positron pairs will produce an additional peak of the photon spectrum at $\sim 31.6\Gamma_{100}$ MeV (Pe'er & Waxman, 2004).

IT IS CLEAR then that observing the VHE component of a GRB would provide a strong constraint on the compactness parameter l' and thus on the fireball Lorentz factor Γ. For fireballs with large compactness, models predict suppresion for energies $\epsilon_\gamma \gtrsim 0.1$ GeV, which is weakly dependent on other parameters. On the other hand, fireballs with small compactness will exhibit emissions above 10 MeV and the low-energy spectrum will depend on ε_B (Pe'er & Waxman, 2004).

2.1.6 *The detectability of each mechanism*

THE RELATIVE importance of the mechanisms described above depends on the equipartition parameters $(\varepsilon_e, \varepsilon_p, \varepsilon_B)$. The effects of these parameters' change to each contribution has been investigated by Gupta & Zhang (2007).

The contribution from electron inverse Compton will decrease as ε_e decreases while ε_B is kept fixed. A low value of ε_e and a high value of ε_p, e.g. $\varepsilon_e/\varepsilon_p \sim 10^{-3}$ will increase the proton syn-

chrotron contribution to the resulting γ-ray spectrum as well as the hadronic component. Pe'er & Waxman (2005) found out that the proton synchrotron emission suggested by Totani (1998b,a) to explain the 1 TeV γ-ray emission from GRB 970417a detected by Milagrito (Atkins et al., 2000b) requires a very low fraction of the energy carried by electrons, $\varepsilon_e \sim 10^{-3}$. This is in contradiction with afterglow observations that imply ε_e to be nearly in equipartition. The explanation favoured by Pe'er & Waxman (2005) is the photoproduction of pion decay, which could be the case if the magnetic field is well below equipartition, $\varepsilon_B \simeq 10^{-4}$.

2.2 *Normalising the observed photon spectrum*

THE PHOTON spectrum of a GRB occuring at redshift z is assumed to be constant during the whole duration of the burst. The burst duration in the observer's frame is $\Delta t = (1+z)\Delta t_*$. The photon spectrum $N(\epsilon)$ of a GRB is approximated by a broken but smoothly connected power law, known as the Band spectrum, which is a model based on BATSE observations of 54 GRB (Band et al., 1993):

Throughout this dissertation, asterisks will be used to indicate terms in the source's frame, while terms without asterisk are terms in the observer's frame

$$N(\epsilon) = f_\gamma \left[H(\epsilon_{\rm bk} - \epsilon) \exp\left(-(b-a)\tfrac{\epsilon}{\epsilon_{\rm bk}}\right) \left(\frac{\epsilon}{\epsilon_{\rm bk}}\right)^{-(a+1)} + H(\epsilon - \epsilon_{\rm bk}) \exp(a-b) \left(\frac{\epsilon}{\epsilon_{\rm bk}}\right)^{-(b+1)} \right] \ \text{TeV}^{-1}\ \text{cm}^{-2}\ \text{s}^{-1}, \tag{2.52}$$

where a and b are respectively the spectral indices of the power law in the low- and high-energy regime demarcated by the break energy $\epsilon_{\rm bk}$, and f_γ is the normalisation constant in unit of photons $\text{TeV}^{-1}\ \text{cm}^{-2}\ \text{s}^{-1}$. The function $H(x)$ is the Heaviside step function defined as $H(x) = 1$ for $x \geq 0$ and $H(x) = 0$ otherwise.

The break energy is related to the directly measurable peak energy $\epsilon_{\rm pk*}$, which is the energy in which the function $\nu f_\nu \equiv \epsilon^2 N(\epsilon)$ peaks, through

$$\epsilon_{\rm bk} = \frac{b-a}{1-a}\epsilon_{\rm pk}. \tag{2.53}$$

Here ν is the frequency of the γ-ray and is related to energy by $\epsilon = h\nu$, where h is the Planck constant.

BATSE observations extend only to several hundreds keV and in some cases to several MeV, but subsequent observations by later satellites confirmed that the power law extends to several GeV (e.g. Hurley et al. 1994; González et al. 2003; Abdo et al. 2009). Based on this we consider the case that this power law function extends to the TeV regime.

The normalisation constant f_γ is calculated by relating the energy spectrum in Equation 2.52 to its instrinsic isotropic-equivalent bolometric luminosity $L^{\rm iso}_{\rm bol*}$:

$$L^{\rm iso}_{\rm bol*} = 4\pi r_c^2(z)(1+z)\int_0^{\Delta t} dt \int_0^{\infty} d\epsilon N(\epsilon)\epsilon, \tag{2.54}$$

in which $r_c(z)$ is its comoving distance at redshift z:

$$r_c(z) = \int_0^z dz'(1+z')\frac{dl}{dz'}, \tag{2.55}$$

where dl/dz is the cosmological line element defined as

$$\frac{dl}{dz} = \frac{c}{H_0}\frac{1}{(1+z)\sqrt{\Omega_\Lambda + \Omega_m(1+z)^3}}, \tag{2.56}$$

in which c is the speed of light, $H_0 = 72\ \mathrm{km\ s^{-1}\ Mpc^{-1}}$ is the Hubble constant at the present epoch, $\Omega_\Lambda = 0.742$ and $\Omega_m = 0.258$ are respectively the present dark energy and matter density in the universe in units of the critical energy density. The critical energy density is related to the Hubble constant H_0 and the gravitational constant G by $3H_0^2/8\pi G$. It is assumed that the GRB emission spectrum is constant during the whole burst duration. It is also important to note that $L^{\rm iso}_{\rm bol*}$ is an isotropic-equivalent luminosity which assumes that the γ-ray emission is isotropic and is not beamed. The true, beamed, bolometric luminosity $L^{\rm true}_{\rm bol*}$ is related to $L^{\rm iso}_{\rm bol*}$ by

$$L^{\rm true}_{\rm bol*} = (1-\cos\theta_j)L^{\rm true}_{\rm bol*}, \tag{2.57}$$

where θ_j is the opening angle of the jet. The average value of the opening angle is $\langle\theta_j\rangle \sim 6^\circ$ (Ghirlanda et al., 2007), making $L^{\rm true}_{\rm bol*} \sim 0.0055 L^{\rm true}_{\rm bol*}$.

The integration in Equation 2.54 can be solved by fixing the spectral index a to the typical value of $a = 0$ (Preece et al. 2000; Natarajan et al. 2005) and letting the other values as free parameters. Solving the integration this way, we can obtain the photon flux f_γ:

$$f_\gamma = \frac{L^{\rm iso}_{\rm bol*}}{4\pi r_c^2(z)\Delta t_* \epsilon^2_{\rm bk*}\lambda_{\rm bol}}, \tag{2.58}$$

in which $\epsilon_{\rm bk*} = \epsilon_{\rm bk}(1+z)$ is the break energy in the source's frame and $\lambda_{\rm bol}$ is a bolometric correction to the flux, which is the result of the integration in energy. To avoid a divergent flux in the integration, we do not integrate it to infinite energy but instead cut the spectrum off at maximum energy $\epsilon_{\rm max*} = 300$ TeV. At the moment the upper cutoff of the photon spectrum is not known, and in fact the taking of 300 TeV as the limit of the integration is quite arbitrary. Taking this in mind, the value of $\lambda_{\rm bol}$ is then

$$\lambda_{\rm bol} = \begin{cases} -\frac{1}{b}\exp(-b) + \frac{1}{b} + \frac{\exp(-b)}{1-b}\left[\left(\frac{\epsilon_{\rm max*}}{\epsilon_{\rm bk*}}\right)^{1-b} - 1\right], & \text{for } b \neq 1 \\ -\frac{1}{b}\exp(-b) + \frac{1}{b} + \exp(-b)\ln\left(\frac{\epsilon_{\rm max*}}{\epsilon_{\rm bk*}}\right), & \text{for } b = 1. \end{cases} \tag{2.59}$$

Thus given $(L^{\rm iso}_{\rm bol*}, z, b, \Delta t_*, \epsilon_{\rm bk*})$ as parameters, we can construct the photon spectrum of any GRB.

2.3 *Photon absorption by ambient infrared photons*

Along the path from the source to the Earth, γ-ray photons interact with extragalactic background light (EBL) through the $\gamma\gamma \to e^+e^-$ process, annihilating themselves and creating pairs of electron-positron. For head-on collisions, the wavelength of EBL photons which will interact with passing TeV photons is then

$$\lambda_{\rm EBL} \simeq \lambda_e \frac{\epsilon_\gamma}{2m_e c^2} = 1.2\left(\frac{\epsilon_\gamma}{1\ {\rm TeV}}\right)\ \mu{\rm m}, \tag{2.60}$$

in which $\lambda_e = h/(m_e c)$ is the Compton wavelength for an electron. We can see that TeV photons will interact strongly with infrared (IR) photons in the EBL.

The optical depth $\tau_{\gamma\gamma}(\epsilon_\gamma, z)$ as a function of observed photon energy ϵ_γ and redshift z can be calculated if we also know the differential number density of background photons $n(\epsilon_{\rm bg}, z)$ at energy $\epsilon_{\rm bg}$ and redshift z:

$$\begin{aligned}\tau_{\gamma\gamma}(\epsilon_\gamma, z) = \tfrac{1}{2}\int_0^z dz \frac{dl}{dz}\int_{-1}^{1} d\mu_i (1-\mu_i) \\ \times \int_{\epsilon_{\rm min}}^{\infty} d\epsilon_{\rm bg} n(\epsilon_{\rm bg}, z)\sigma[\epsilon_\gamma(1+z), \epsilon_{\rm bg}, \mu_i],\end{aligned} \tag{2.61}$$

in which $\epsilon_{\rm min} = \epsilon_{\rm th}(1+z)^{-1}$, $\frac{dl}{dz}$ is the cosmological line element defined in Equation 2.56, and $\sigma(\epsilon_1, \epsilon_2, \mu_i)$ is the cross section of the $\gamma\gamma$ pair production.

Directly observing EBL photons to obtain their photon distribution is difficult because of contamination issue from the instrument as well as from the zodiacal light. Source discrimination is also another issue: The Cosmic Infrared Background (CIB)—which is extragalactic in nature—must be discriminated from foreground objects such as discrete sources like stars and compact objects within the Galaxy, as well as diffuse sources such as light scattered and emitted by interplanetary dust and emission by interstellar dust (see Hauser & Dwek (2001) for a review on this matter).

There are many approaches in calculating the EBL photon density for all redshifts. One basic approach of doing it is by using "backward models," in which we start from the existing galaxy count data and then model the luminosity evolution of these galaxies backward in time (e.g. Stecker, Malkan & Scully 2006). Another approach is the "forward evolution," performed by assuming a set of cosmological theory and semi-analytic merger-tree models of galaxy formation to determine the star formation history of the universe (e.g. Primack, Bullock & Somerville 2005; Gilmore et al. 2009). Yet another approach is to focus on the properties and evolution of starlight, the primary source of CIB emission. This model integrates stellar formation rates and properties over time to obtain the amount of light emitted (e.g. Kneiske et al. 2004; Finke, Razzaque & Dermer 2010).

In this dissertation three different attenuation models are considered: The "best-fit" model of Kneiske et al. (2004), the fidu-

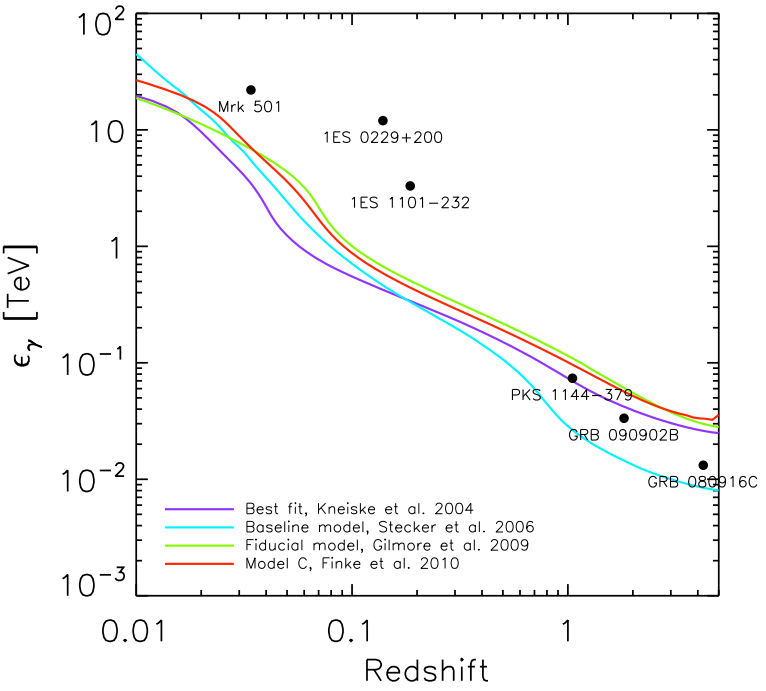

Figure 2.2: A plot of the Fazio-Stecker Relationship (Fazio & Stecker, 1970) for several attenuation models, as a function of redshift. Also shown are the redshifts and highest energy photons $\epsilon_{\max}$ of various objects observed by Atmospheric Čerenkov Telescopes and *Fermi*-LAT (Finke & Razzaque, 2009; Abdo et al., 2010).

cial model of Gilmore et al. (2009), and the recent "Model C" by Finke, Razzaque & Dermer (2010). These models, along with the Baseline Model of Stecker, Malkan & Scully (2006), are compared in the plot of the Fazio-Stecker relation (Fazio & Stecker, 1970) in Figure 2.2. The Fazio-Stecker relation is the (ϵ_γ, z) value that gives $\tau_{\gamma\gamma} = 1$. This is interpreted to be the redshift at which the flux of photons of a given energy is attenuated by a factor e and is called the γ-ray horizon. In this plot, for all models except those of Stecker, Malkan & Scully (2006), for redshift $\lesssim 5$ the universe is optically thin to photons with energy $\lesssim 20$ GeV. At very low redshifts however, the models are relatively consistent with each other, but the differences start to become apparent at $z \gtrsim 1$. The model calculated by Stecker, Malkan & Scully (2006), which predicts higher attenuation at higher redshifts, has in recent times contradicted MAGIC (Albert et al., 2008) and *Fermi* (Abdo et al., 2010) observations and thus can be ruled out with high con-

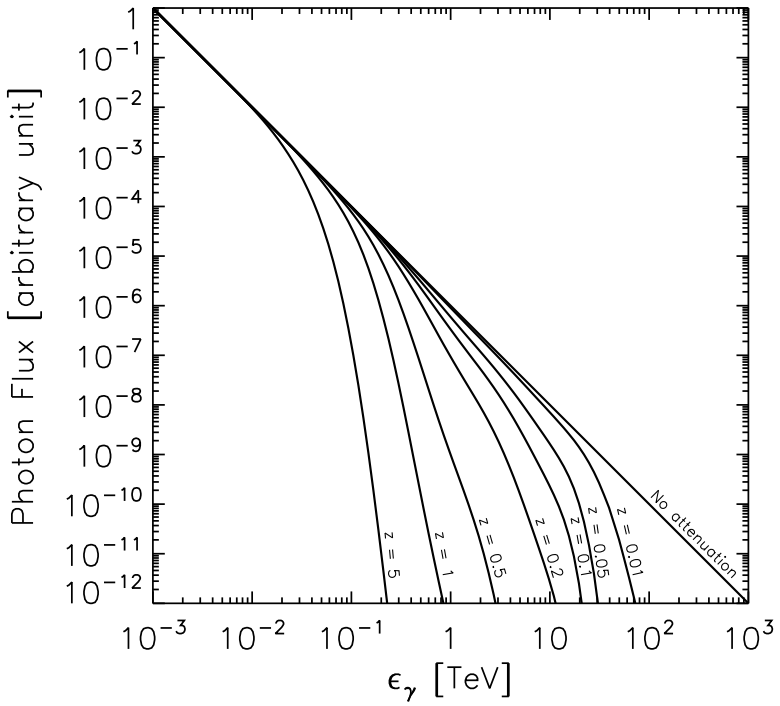

Figure 2.3: An illustration of the effect of attenuation to a photon spectrum. Attenuation is calculated using the model by Finke, Razzaque & Dermer (2010). The shape of the photon spectrum of a source located at redshifts indicated beside each curve is shown. Energies are in the observer frame of reference. The further a source is located, more attenuation is suffered by the highest energy photons. The curve is normalized to unity at $\epsilon_\gamma = 1$ GeV.

fidence (furthermore, Figure 3 in Abdo et al. (2010) indicate that models by Finke, Razzaque & Dermer (2010); Gilmore et al. (2009); Franceschini, Rodighiero & Vaccari (2008) are the favourable ones) and will not be used in further calculations.

Thus, knowing the attenuation function, we can then estimate the total number of photons emitted from a GRB at redshift z per unit energy arriving at the top of the Earth's atmosphere per unit area per unit time to be

$$\gamma_0(\epsilon_\gamma) = \gamma(\epsilon_\gamma, t = 0) \equiv f_\gamma \left(\frac{\epsilon_\gamma}{\epsilon_{\rm bk}} \right)^{-(b+1)} e^{-\tau_{\gamma\gamma}(\epsilon_\gamma, z)}, \qquad (2.62)$$

where f_γ is as derived in Equation 2.59 and $\gamma(\epsilon, t)$ is the notation for the photon flux at slant depth t in the atmosphere, as introduced in Rossi & Greisen (1941). Slant depth $t = 0$ means the top of the atmosphere. In this equation only the high-energy part of Equation 2.52 is used, because this is precisely the concern of this

study and henceforth this equation will be the working equation.

To give an illustration of the effect of attenuation to a photon spectrum, the shape of the photon spectrum curve of several sources emitting at different redshifts is showed in Figure 2.3. As a comparison an unattenuated photon spectrum is also shown. The curves are normalized to an arbitrary unit. From the shape of the curves, the more distant the source is located, the more the photon spectrum curve is distorted due to attenuation effects. This imposes a limit on the number of TeV photons that we can observe from a given source.